J Polym Res (2014) 21:480
DOI 10.1007/s10965-014-0480-x

ORIGINAL PAPER

Preparation and characterization of melamine-based porous Schiff base polymer networks for hydrogen storage

Rasha A. El-Ghazawy · Abdallah G. Mahmoud · M. João Ferreira · Clara S. B. Gomes · Pedro T. Gomes · K. A. Shaffei · Ayman M. Atta

Received: 18 February 2014 / Accepted: 9 May 2014

Abstract Based on Schiff base chemistry, crosslinked porous organic aminal networks were prepared using acetic acid as a catalyst. These Schiff base networks (SNWs) are polymeric materials based on melamine and 5,5′-methylene-bis-salicylaldehyde, with nitrogen contents as high as *ca*. 36 wt.%, which were characterized by FTIR spectroscopy, elemental analysis, and ^{13}C and ^{15}N solid-state NMR spectroscopies. A series of polymer networks with different monomeric molar ratios and different amounts of added catalyst were explored, in order to study their effect on the final polymer structure, porosity and H_2 storage capacity. These materials exhibit Brunauer-Emmett-Teller (BET) surface areas up to *ca*. 526 m^2/g, as measured by N_2 adsorption at 77 K, and exhibit gravimetric storage capacities up to 2.57 wt.% at 20 bar and 77 K.

Keywords Aminal networks · Hydrogen storage · Melamine-based networks · Porous polymers · Schiff base networks

Electronic supplementary material The online version of this article (doi:10.1007/s10965-014-0480-x) contains supplementary material, which is available to authorized users.

A. G. Mahmoud · M. J. Ferreira · C. S. B. Gomes · P. T. Gomes (✉)
Centro de Química Estrutural, Departamento de Engenharia Química, Instituto Superior Técnico, Universidade de Lisboa, Av. Rovisco Pais, 1049-001 Lisboa, Portugal
e-mail: pedro.t.gomes@tecnico.ulisboa.pt

A. G. Mahmoud · K. A. Shaffei
Department of Chemistry, Faculty of Science, Helwan University, Ain Helwan, Cairo, Egypt

R. A. El-Ghazawy · A. M. Atta
Egyptian Petroleum Research Institute, 1 Ahmad Elzomor St., Nasr City, 11727 Cairo, Egypt

A. M. Atta (✉)
Surfactant Research Chair, Chemistry Department, College of Science, King Saud University, P.O. Box 2455, 11451 Riyadh, Saudi Arabia
e-mail: aatta@ksu.edu.sa

Introduction

The widespread use of hydrogen as a fuel is limited by the lack of convenient, cost-effective, and safe methods for H_2 storage [1, 2]. The U.S. Department of Energy (DOE) targets for onboard automotive hydrogen storage have slightly varied in the last 13 years [1–3], the gravimetric and volumetric targets for 2017 being defined as 5.5 wt.% and 40 g H_2/L, respectively [4]. These targets are very challenging because the calculations of H_2 storage capacity involve pressure and temperature. Generally, the H_2 capacity of a material increases with increasing pressure and decreasing temperature, but the uses of elevated pressure (with the necessary containment technology) or low temperature (with the associated cooling system) will generally increase the system cost and weight, and hence will decrease the system efficiency.

Materials such as metal hydrides [2], zeolites [5, 6], metal-organic frameworks (MOFs) [2], activated carbon [2, 7, 8], carbon nanotubes [2, 9, 10], and porous polymers [2, 11–13] have been among the most studied substances for hydrogen storage. In particular, research in porous organic polymers have been a very interesting topic in the recent years due to the wide variety of applications including gas storage [11–15], sorption of organic vapors [16, 17], gas separation [18], and heterogeneous catalysis [19, 20]. They have several advantages such as: a wide variety of organic reactions that can be used to prepare and modify them, they are composed of light elements such as C, H, N, and O, they avoid the inclusion of high molecular weight metals, and they tend to be insensitive to ambient air, easy to handle and mechanically stable [21].

Published online: 17 May 2014

Various types of porous organic polymers have been developed for H_2 storage applications, including covalent organic frameworks (COFs), polymers of intrinsic microporosity (PIMs), and hypercrosslinked polymers (HCPs) [21]. COFs are composed of organic molecules linked together by means of covalent bonds forming crystalline porous networks [11, 22] that may exhibit H_2 storage capacities up to 1.7 wt.% H_2 at 77 K, and 1 bar [23]. PIMs are polymers with a highly rigid molecular structure, in which the pores are provided by the macromolecular subunits that cannot pack space efficiently [24], having been demonstrated to adsorb up to 2.7 wt.% H_2 at 77 K, and 10 bar [25]. HCPs represent a very important class of organic polymer materials with high surface areas, in which the permanent porosity is provided by the extensive chemical crosslinking [12, 13, 26], and exhibiting hydrogen storage capacities up to 3.7 wt.% at 77 K, and 15 bar [13].

Several methods have been established for the generation of porous organic polymers, but most of them often rely on expensive and complex building blocks and/or the need of costly noble metal catalysts or strong Lewis acid catalysts [24, 27, 28]. Therefore, it is a great challenge to synthesize porous organic polymers using cheap and simple processes.

Melamine (MA), 66 % N by mass, is a cheap triazine compound used in many fields such as plastic, medicinal, decorative, and paper industries. It also has been used to produce N–enriched porous materials [15, 29–31] that can be used in several applications including hydrogen storage. In a recent work, Schwab et al. developed a new class of N–enriched porous polymer networks, namely Schiff base networks (SNWs), with relative high surface area using a novel one-pot method through Schiff base chemistry by condensation of MA with several aromatic aldehydes in dimethyl sulfoxide (DMSO) [31]. They found that the produced polymer structure was that of an aminal (−HN–C–NH–) network rather than an iminic (−C = N–) one. This can be understood taking into consideration the chemistry of imines, in which an imine double bond can further react with primary amines, resulting in the production of aminal groups [32]. Significant progress has been made in the development of organic networks through Schiff base chemistry using different kinds of amine and aldehyde structures to produce a wide variety of porous organic networks with different surface areas and different applications [33–38]. Very recently, in 2014, Li et al. reported the preparation of crystalline imine-linked Schiff base polymers based on tetraphenyladamantane [39], using the synthetic technique of Schwab et al. [31]. These polymer networks exhibit BET surface areas and H_2 uptakes of up to 1,045 m^2/g and 1.26 wt.%, respectively, at 77 K and 1 bar [39].

The aim of the present work is the preparation of a new N-enriched porous organic network through Schiff base chemistry, by a facile polycondensation reaction involving simple chemical reagents, such as MA and 5,5′-methylene-bis-salicylaldehyde (DA), to be used for hydrogen storage. The structures and properties of the resulting materials were systematically characterized by various adequate techniques. To the best of our knowledge, this is only the second example (besides that of Li et al. [39]) where a Schiff base network is tested for hydrogen storage.

Experimental

General

Starting materials and solvents were obtained from commercial sources (e.g. Alfa Aesar) and used as received without further purifications. DMSO, used as solvent to prepare SNWs, was dried as described by Armarego and Chai [40], the DMSO being allowed to stand for a week with pre-activated molecular sieves of type 4 Å, and subsequently distilled over CaH_2 under reduced pressure. The dry DMSO was stored under nitrogen atmosphere.

All operations performed under nitrogen gas were carried out using a dual vacuum/nitrogen line and standard Schlenk techniques. Nitrogen gas was supplied in cylinders (Air Liquide) and purified by passage through 4 Å molecular sieves.

The synthesized starting material (DA) was characterized by solution Nuclear Magnetic Resonance (NMR) spectroscopy, the spectra being recorded on a Bruker Avance III 300 (^1H and ^{13}C) spectrometer. Spectra were referenced internally to residual protio-solvent (^1H) or solvent (^{13}C) resonances and are reported relative to tetramethylsilane ($\delta=0$). All chemical shifts are quoted in δ (ppm) and coupling constants given in Hz. Multiplicities were abbreviated as follows: singlet (s) and doublet (d). Elemental analyses were obtained from the Instituto Superior Técnico elemental analysis services.

Synthesis of 5,5′-methylene-bis-salicylaldehyde (DA)

The synthesis of DA was adapted from a procedure described in the literature [41]. To a solution of 17.2 mL (20 g, 0.163 mol) of salicylaldehyde in 12.5 mL of glacial acetic acid (Ac), in which 1.75 g (0.019 mol) of trioxane was dissolved, a mixture of 0.12 mL of concentrated sulfuric acid and 0.6 mL of glacial acetic acid was added slowly with magnetic stirring under nitrogen atmosphere, at a temperature of 90–95 °C. This temperature was maintained for 22 h, and stirring continued over the whole reaction period. The reaction mixture was allowed to stand in an ice bath overnight. The deposited solid was filtered, and extracted twice with 25 mL of petroleum ether. The isolated solid was then three times ground with 20 mL of diethyl ether and the supernatant ether solutions were decanted. Finally, the solid was recrystallized from 40 mL of acetone. Yield, 9.41 g (45 %).

FTIR (KBr, selected bands): ν (cm^{-1})=3,435 (m) (O–H); 2,925 (w), 2,850 (w) (C–H, methylene); 1,660 (s) (C=O); 1,600 (m), 1,588 (w), 1,447 (w) (C=C); 830 (w), 811 (w) δ(C–H, aromatic).

^{1}H NMR (300 MHz, $CDCl_3$): δ=10.92 (s, 2H, O*H*), 9.85 (s, 2H, C*H*=O), 7.36 (d, $^3J_{HH}$=7.5 Hz, 2H, $CH_2CC(H)C$), 7.33 (s, 2H, HOCCHC*H*), 6.95 (d, $^3J_{HH}$=7.5 Hz, 2H, HOCC*H*CH), 3.96 (s, 2H, CH_2). $^{13}C\{^1H\}$ NMR (75 MHz, $CDCl_3$): δ=196.56 (O=*C*H), 160.44 (HO*C*), 137.75 (CH_2CCHCH), 133.37 (O=CHC*C*H), 132.11 (O=CH*C*), 120.64 (CH_2C), 118.18 (HOC*C*H), 39.56 (*C*H_2).
Elemental analysis: calcd (%) for $C_{15}H_{12}O_4$: C 70.31, H 4.72; found: C 70.76, H 4.97.

Preparation of SNWs with different monomeric molar ratios

A Schlenk tube fitted with a condenser and a magnetic stir bar was charged with DA (0.5 g, 2 mmol), MA (1.3, 4, 6, 8 or 14 mmol to produce SNW-Q, SNW-R, SNW-S, SNW-T or SNW-U, respectively), dry DMSO (5 mL) and glacial acetic acid (16 mmol). After degassing by nitrogen bubbling, the mixture was heated to 180 °C for 72 h, under an inert atmosphere, with continuous stirring. After cooling to room temperature the precipitated network was isolated by filtration and washed with acetone, ethanol and dichloromethane. The remaining solvent was removed under vacuum at 60 °C to afford the materials as yellow powders. Yields: SNW-Q, 0.32 g; SNW-R, 1.14 g; SNW-S, 1.53 g; SNW-T, 1.97 g; SNW-U, 2.94 g.

Preparation of SNWs with different DA to catalyst molar ratios

The synthesis of this set of SNWs was performed as described above, the amount of MA used being 0.5 g (4 mmol), whereas the amounts of glacial acetic acid used were 1, 2, 4, 8, and 16 mmol to produce SNW-V, SNW-W, SNW-X, SNW-Y and SNW-R, respectively. Yields: SNW-V, 1.21 g; SNW-W, 1.23 g; SNW-X, 1.27 g; SNW-Y, 1.18 g; SNW-R, 1.14 g.

Characterization of SNWs

Elemental analysis: C, H and N elemental analyses were carried out by the elemental analysis services of the Instituto Superior Técnico.

Fourier transform infrared (FTIR): Infrared spectra (4,000–400 cm^{-1}) were recorded on a Jasco FT/IR-4100 instrument as KBr pellets.

Solid state NMR: Solid-state NMR spectra were measured on a TecMag/Bruker 300 "wide bore" spectrometer. For cross-polarization magic angle spinning (CP-MAS) ^{13}C NMR spectrum, the employed frequency was 75.49 MHz, the magic angle spinning rate was 3.8 kHz, the contact time was 3 ms, the relaxation delay was 3 s, and the external reference used was Glycine. For CP-MAS ^{15}N NMR spectrum, the employed frequency was 30.42 MHz, the magic angle spinning rate was 3.8 kHz, the contact time was 3 ms, the relaxation delay was 3 s, and the external reference used was Glycine. All spectra were acquired at room temperature. The analysis of the spectra was carried out using Tecmag software.

Thermal gravimetric analysis of SNWs

Thermal gravimetric analysis (TGA) measurements were examined using a SDT 2960 Simultaneous DSC-TGA equipment, from room temperature to 800 °C, and a heating rate of 10 °C min^{-1}, under N_2.

Sorption isotherms: surface areas, total pore volumes, and H_2-uptakes

The specific surface area (BET) and total pore volume (PV) of the polymers were determined from nitrogen adsorption isotherms, measured at 77 K, using a Quantachrome NOVA Automated Gas sorbometer (NOVA 2200e). All samples were degassed at 150 °C under dynamic vacuum overnight before performing the tests.

The measurements of the hydrogen storage capacities of samples were determined at 77 K, over a pressure range up to 20 bar, with an Intelligent Gravimetric Analyzer (IGA-003, Hiden) that incorporates a microbalance capable of measuring weights with a resolution of ±0.2 μg. Degassing of all polymers was performed at 150 °C under dynamic vacuum, overnight, before performing the test.

Results and discussion

Synthesis of the dialdehyde

The monomeric dialdehyde, 5,5′-methylene-bis-salicylaldehyde (DA), was prepared in 45 % yield, as reported in the experimental section, by treating salicylaldehyde with trioxane in acetic acid, in the presence of sulfuric acid as catalyst. Using this procedure, proposed by Marvel and Tarköy [41], the yield of dialdehyde depends mainly on the amount of sulfuric acid catalyst used, which can be understood from the assumption that the salicylaldehyde to formaldehyde ratio must be very high in order to promote the formation of dialdehyde instead of a polymeric product. It has been shown that the rate of acid-catalyzed depolymerization of trioxane to formaldehyde bears a close correlation to the acid concentration of the reaction medium [42]. Thus, a

low acid concentration keeps the ratio of salicylaldehyde to formaldehyde favorable for the dialdehyde preparation.

Synthesis of the Schiff base networks (SNWs)

Melamine (MA) and DA were employed to prepare the target SNWs by Schiff base polycondensation, using the procedure described in the experimental part. The synthetic reaction used to prepare MA-based porous polymers is depicted in Scheme 1.

As the mechanism of Schiff base reaction involves a number of reversible steps, the solvent used, DMSO, should be dried to improve the reaction kinetics. Due to the intramolecular forces between the neighboring hydroxyl and aldehyde groups, the aldehyde group needs to be activated for Schiff base condensation. Therefore, we chose acetic acid because of the mechanism of DA activation proposed by Marvel and Tarköy [42].

At high temperature, DMSO is thermally decomposed to formaldehyde, dimethyl sulfide, methyl mercaptane and water [43]. The formaldehyde produced can react with free amino groups of MA to form methylol groups. These methylol groups undergo condensation, especially at low DA:MA ratios, forming crosslinks via two types of linkages: an ether linkage and a methylene linkage, similar to those observed in MA resins (Scheme 2) [44–46].

Structural analysis of SNWs

The conversion of the functional groups of the monomers, and successful production of polymeric networks, was confirmed by Fourier transform infrared (FTIR) spectroscopy. As shown in Fig. 1, the absence or sharp decrease in the intensity of bands attributed to the primary amine groups of MA at 3,469 and 3,419 cm^{-1} (NH_2 stretching), and bands corresponding to the formyl function of DA at 1,660 cm^{-1} (C=O stretching), gives an indication of successful condensation reaction between amino and aldehyde groups. The broad band appearing at 3,435 cm^{-1} corresponds to O–H stretching of hydroxyl group of DA that remained in the structure of the SNW produced. The bands appearing at 2,925 and 2,850 cm^{-1} are

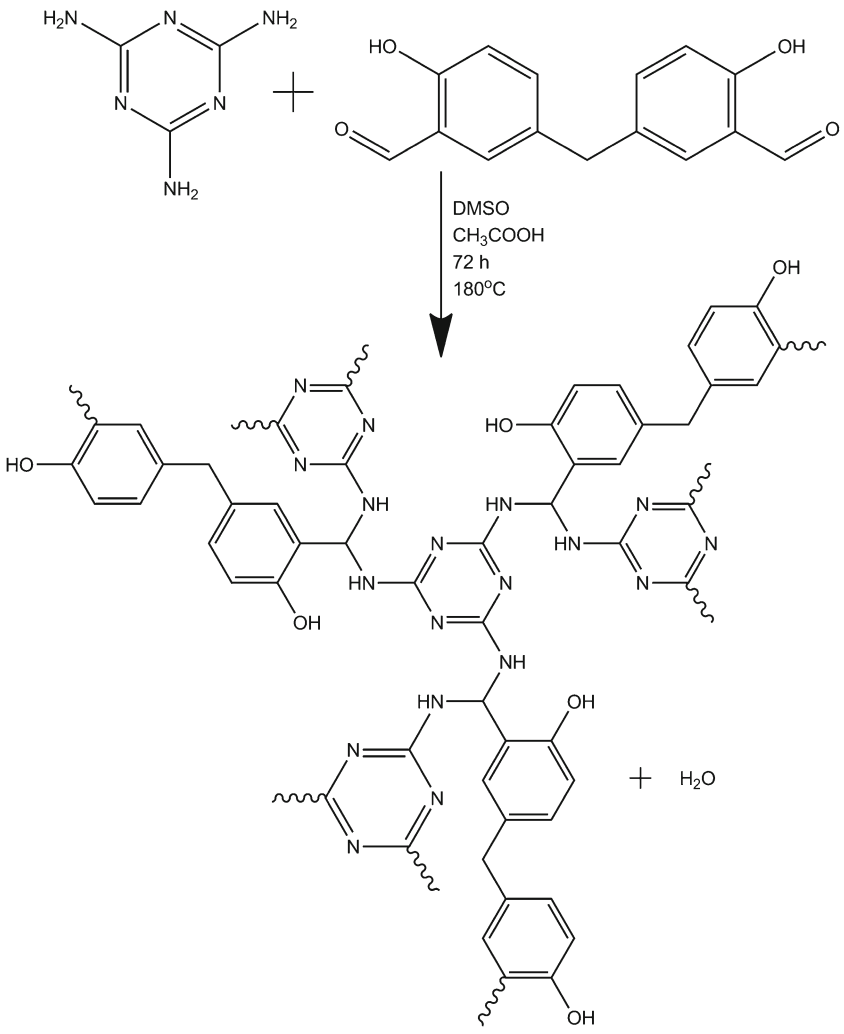

Scheme 1 Synthesis of SNWs by Schiff base condensation of MA and DA

Scheme 2 Formation of methylene and ether linkages

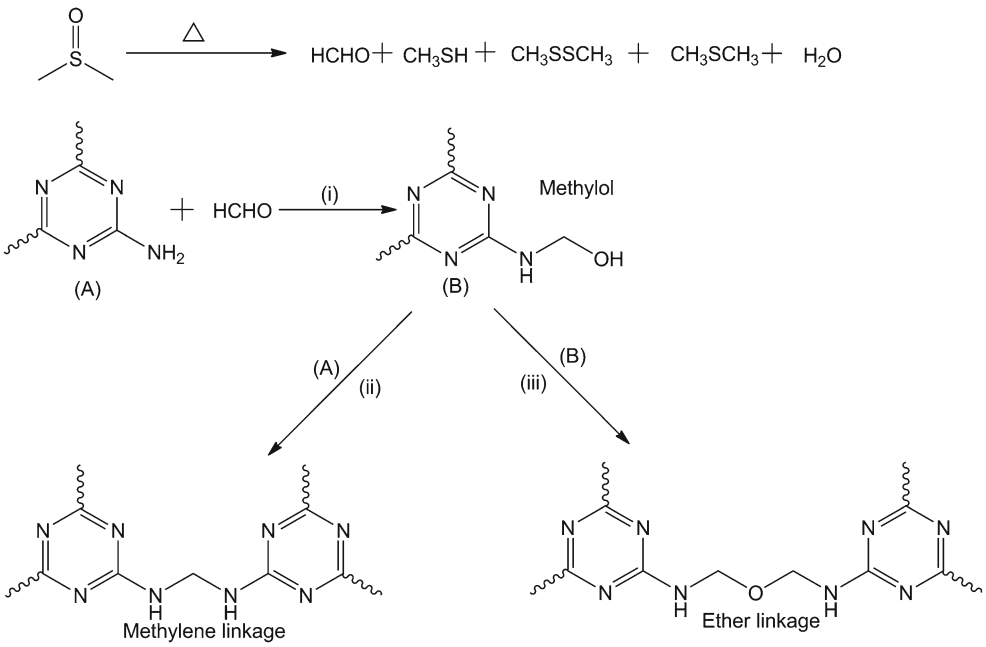

attributed to C–H stretching of the methylene linkages of DA that remained unchanged in the final SNW structure. The presence of distinct bands attributed to triazine ring quadrant stretching vibrations (1,540 cm^{-1}) and semi-circle stretching vibrations (1,450 cm^{-1}) indicates the successful incorporation of MA into the network structure [47]. Finally, the absence of aromatic aldimine groups (Ar–C=N–) in all SNWs produced can be confirmed because no C=N stretching bands are visible at 1,613–1,640 cm^{-1} [32, 34, 48].

The required DA:MA molar monomeric ratio for complete condensation of $–NH_2$ and –CHO groups can be determined by FTIR spectroscopy. The spectrum of the SNW obtained with the highest DA:MA ratio (3:2) shows a strong band at 1,660 cm^{-1}, which corresponds to unreacted C=O groups, meaning that the amount of MA added to the reaction is not enough for complete condensation with DA units. As the monomeric DA:MA ratio decreases (amount of MA used in the reaction increases), the band at 1,660 cm^{-1} decreases and

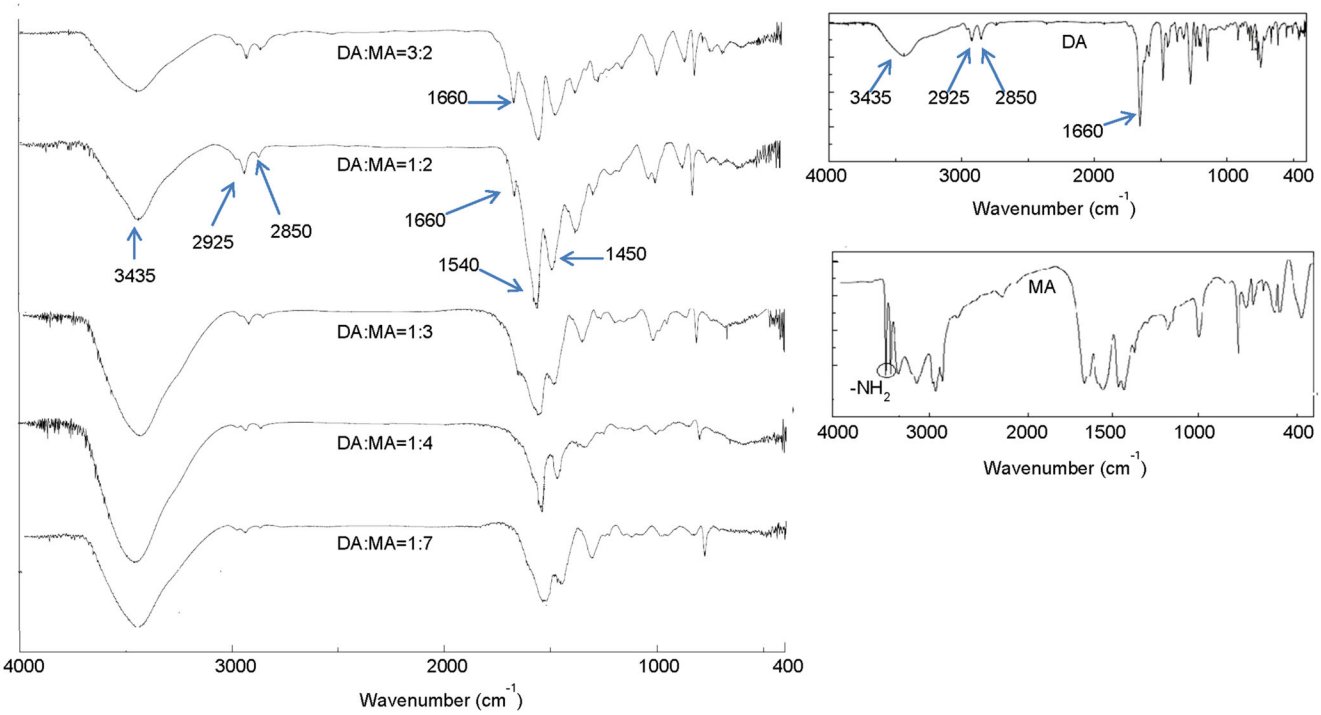

Fig. 1 FTIR spectra of DA and MA monomers (right) and of SNWs produced with different DA:MA molar ratios (left)

disappears completely when the DA:MA molar ratio used in the reaction becomes lower than 1:3. Therefore, we can assure that the DA:MA molar ratio should be lower than 1:3 for complete condensation between $–NH_2$ and –CHO groups.

The detailed analysis of the chemical structure of SNWs was performed by ^{13}C and ^{15}N solid-state NMR spectroscopy due to the poor solubility of SNW polymers in common solvents.

The CP-MAS ^{13}C NMR spectrum of SNW-S is shown in Fig. 2. The strong resonance at 166.7 ppm corresponds to the aromatic carbons of the triazine ring. The resonance appearing at 39.5 ppm can be attributed to the methylene linkage between the aromatic rings belonging to DA monomeric units. The resonance at 54.1 ppm can be assigned to the tertiary carbon atoms formed upon addition of the primary amine groups of MA to the newly formed C=N bond leading to aminal structures [32], but this peak is not very sharp because the methylene linkage produced from the reaction of MA with formaldehyde (Scheme 2, reaction ii) shows a resonance in the region of 40–60 ppm [44, 49, 50]. The resonances in the region of 115–140 ppm (plus the resonance at 151.9 ppm, which is deshielded due to the presence of the adjacent O–H group) are assigned to the aromatic carbons of the benzene ring. The 60–80 ppm region corresponds to the carbon atoms present in the methoxy functions, which are produced in the reaction of MA with formaldehyde (Scheme 2, reactions i and iii) [49–51]. The absence of a C=N resonance at 160 ppm confirms the absence of imine bonds in the polymer structure [34, 49]. Conversely, the absence of a carbonyl resonance at 194 ppm assures the absence of DA precursor in the final product, indicating the complete condensation between –CHO and $–NH_2$ groups. In summary, the CP-MAS ^{13}C NMR spectrum clearly indicates the formation of an aminal-linked network instead of an imine-linked one, which is in good agreement with the literature data concerning the aminal-linked networks [31, 38].

The CP-MAS ^{15}N NMR spectrum of sample SNW-S is shown in Fig. 3. The resonance at −280.6 ppm is assigned to the secondary amine nitrogens present in the aminal structure between triazine and aromatic rings. The resonance at −204.2 ppm corresponds to the nitrogen atoms in triazine ring. The assumption of aminal structure formation instead of imine one is strongly supported by the absence of a resonance typical of C=N imine nitrogens at *ca.*–55 ppm [31].

Effect of the variation of monomeric molar ratio on the SNW structure

To study the effect of DA:MA molar ratio change on the ultimate SNW structure, different SNW samples were prepared with DA:MA ratios ranging from 1:2 to 1:7. The variation in composition, and thus the final structure can be observed by performing elemental analyses (C, H, and N) to all the SNW samples. As shown in Table 1, the nitrogen to carbon atomic ratio (N:C) increases with a decrease in the DA:MA monomeric ratio. This means that the higher the amount of MA added to the reaction media, the more successful inclusion of MA units into the polymer network. The assumption of formation of different linkages (methylene and ether linkages, Scheme 2) is strongly supported regarding the complete condensation of $–NH_2$ (from MA units) and

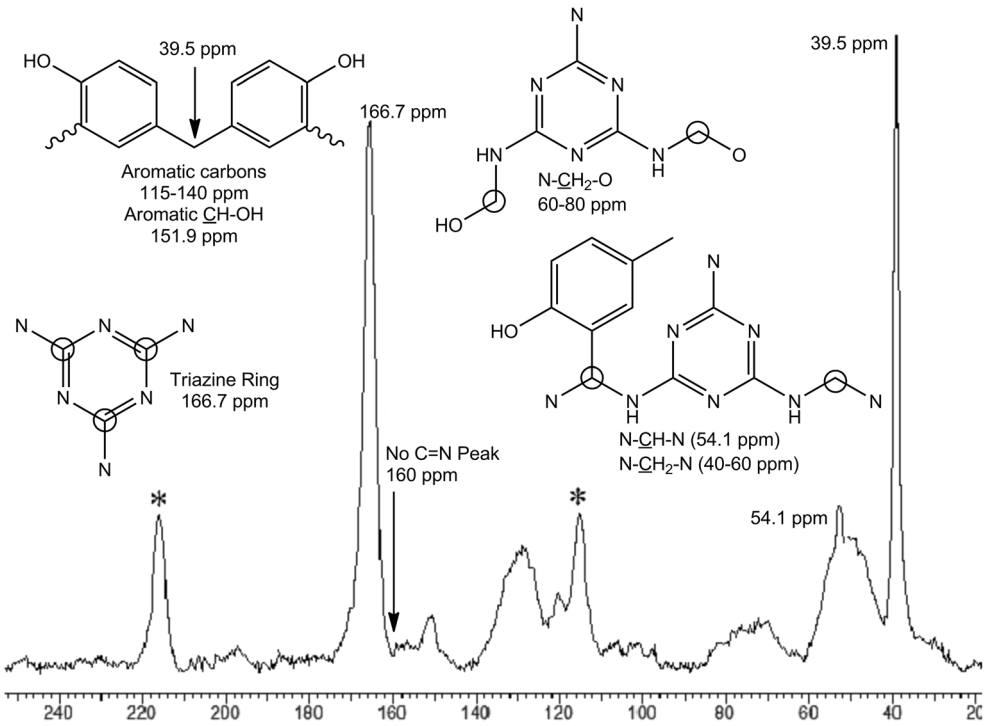

Fig. 2 CP-MAS natural abundance ^{13}C NMR spectrum of sample SNW-S. The asterisks denote the rotational sidebands

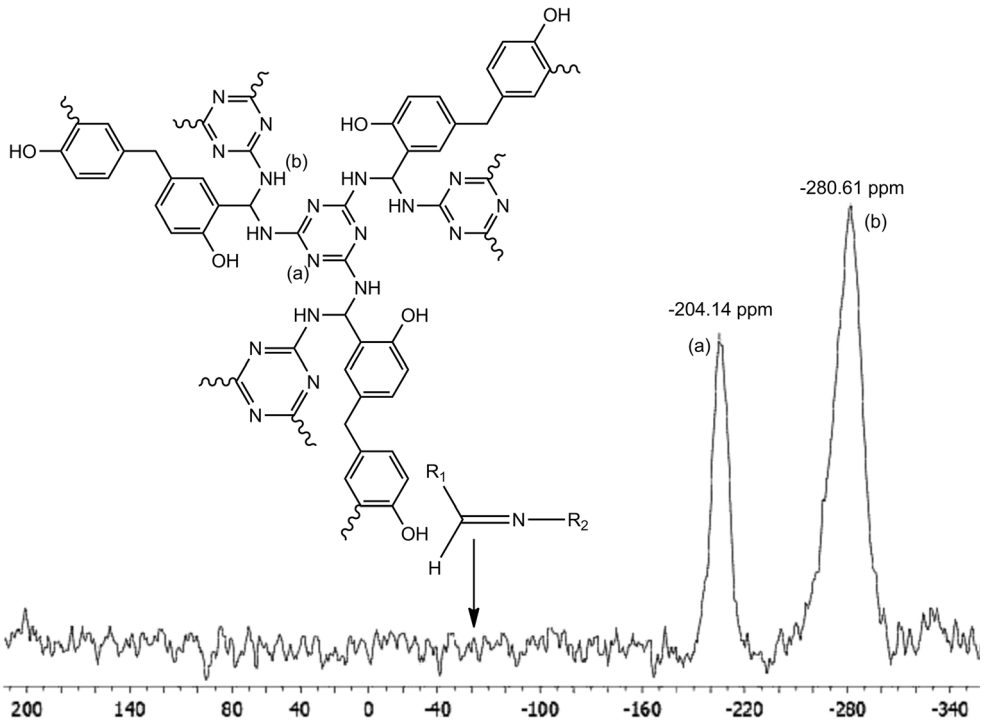

Fig. 3 CP-MAS natural abundance ^{15}N NMR spectrum of sample SNW-S

–CHO (from DA units) groups at DA:MA molar ratio below 1:3, as previously proved by the FTIR spectra taken at different molar ratios, whereas the elemental analyses data show that MA units are still merging into the SNW structure at molar ratios below 1:3.

Thermal stability

Because the prepared porous materials must be outgassed prior to surface area and H_2 uptake measurements, thermal stability studies have been carried out. TGA curves of the SNWs are displayed in Fig. 4. The polymers show a small weight loss before 300 °C, and then a major decomposition after 380 °C. The gradual mass loss before 300 °C can be attributed to outgassing of moisture and solvent (DMSO) trapped inside the networks, the dehydration between methylol groups upon heating, and the post-polycondensation process of amine with formyl end groups that continue at high temperature to react and expel water [52].

Table 1 Chemical elemental analyses of the SNW polymers resulting from different DA:MA molar ratios

Sample	DA:MA	Elemental analysis			N:C [b]
	molar ratio [a]	N %	C %	H %	
SNW-R	1:2	23.55	46.43	5.01	0.51
SNW-S	1:3	26.23	43.73	5.12	0.60
SNW-T	1:4	30.34	44.23	4.73	0.69
SNW-U	1:7	36.13	42.73	4.79	0.85

[a] Monomer molar ratio. [b] Nitrogen to carbon atomic ratio

Porous properties and H_2 storage capacity of SNW materials

Generally, the incorporation of rigid moieties into network structures is beneficial for permanent porosity generation in polymers [25, 53, 54]. As the primary aim of this study was to identify polymer networks with gravimetric hydrogen storage properties, different reaction conditions, mainly monomeric molar ratio and amount of catalyst, were explored to identify the conditions for optimum pore structure and high specific surface area to maximize hydrogen sorption properties (Table 2, entries 1–10). These results show that the synthesis conditions have a great influence on the quantity of hydrogen adsorbed by the material. However, the specific surface areas

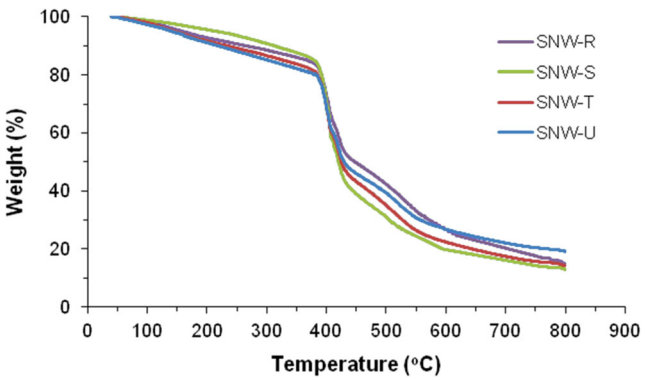

Fig. 4 TGA curves of SNW polymers

Table 2 Synthesis conditions, surface areas, and gravimetric H_2 uptakes for SNWs

Entry no.	Sample	DA:MA [a]	DA:Ac [b]	BET surface area (m^2/g)	PV [c] (cm^3/g)	H_2 uptake (1/20 bar) (wt.%)
1	SNW-Q	3:2	1:8	138.7	0.17	0.38/0.73
2	SNW-R	1:2	1:8	177.1	0.35	0.46/1.06
3	SNW-S	1:3	1:8	379.5	0.53	0.64/1.86
4	SNW-T	1:4	1:8	297.5	0.34	0.54/1.64
5	SNW-U	1:7	1:8	163.6	0.29	0.41/1.06
6	SNW-V	1:2	2:1	252.7	0.46	0.52/1.32
7	SNW-W	1:2	1:1	313.5	0.41	0.63/1.73
8	SNW-X	1:2	1:2	301.9	0.48	0.57/1.69
9	SNW-Y	1:2	1:4	222.2	0.38	0.51/1.25
10	SNW-Z	1:3	1:1	525.8	0.64	0.82/2.57

[a] Monomers molar ratio (Dialdehyde to Melamine). [b] Dialdehyde to Catalyst (Acetic acid) molar ratio. [c] Total pore volume calculated from nitrogen adsorption at P/P_o=0.95

of SNWs of this work are somewhat lower than those reported by Schwab et al. [31].

The porous properties of the SNW materials were analyzed, after degassing the corresponding samples at 150 °C under dynamic vacuum, by nitrogen adsorption-desorption isotherms (Fig. 5), whereas the hydrogen storage capacity of each network sample was determined from hydrogen sorption isotherms at 77 K and pressures up to 20 bar (Fig. 6).

As shown in Fig. 5, the SNW samples present type IV isotherms, which are characteristic of mesoporous adsorbents, being associated with capillary condensation occurring in mesopores [55].

The H_2 sorption isotherms of SNW samples are represented in Fig. 6, and show good reversibility and absence of hysteresis. It is also clear that H_2 uptake does not approach saturation even at a pressure of 20 bar, implying that even greater uptake capacities are possible at more elevated pressures.

To study the monomeric molar ratio effect, many SNW networks with different DA:MA ratios were explored. As indicated in Table 2, entries 1–5 (and shown in Fig. S1 in Electronic Supplementary Material), when the DA:MA molar ratio decreases the BET surface area together with the total pore volume (PV) increase up to *ca.* 379 m^2/g and *ca.* 0.53 cm^3/g, respectively, which corresponds to a DA:MA ratio of 1:3 (entry 3). A decrease in the DA:MA ratio below 1:3 (entries 4 and 5) sharply decreases the BET surface area. This

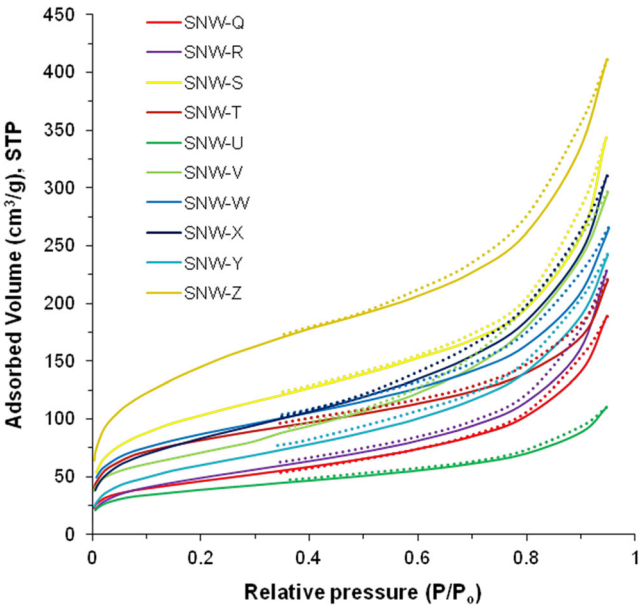

Fig. 5 Nitrogen adsorption-desorption isotherms observed for the SNW samples. Solid lines for adsorption and dotted lines for desorption

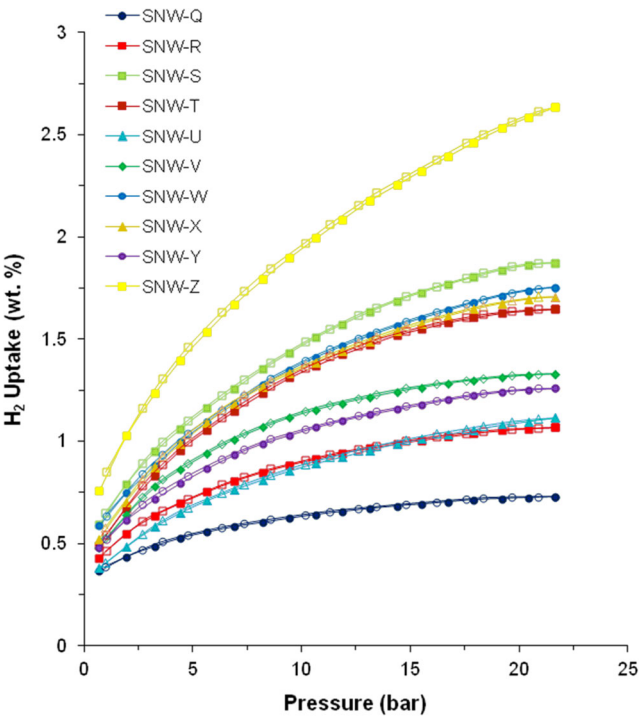

Fig. 6 Gravimetric H_2 sorption isotherms observed for the SNW samples up to 20 bar at 77 K. Solid markers for adsorption and hollow markers for desorption

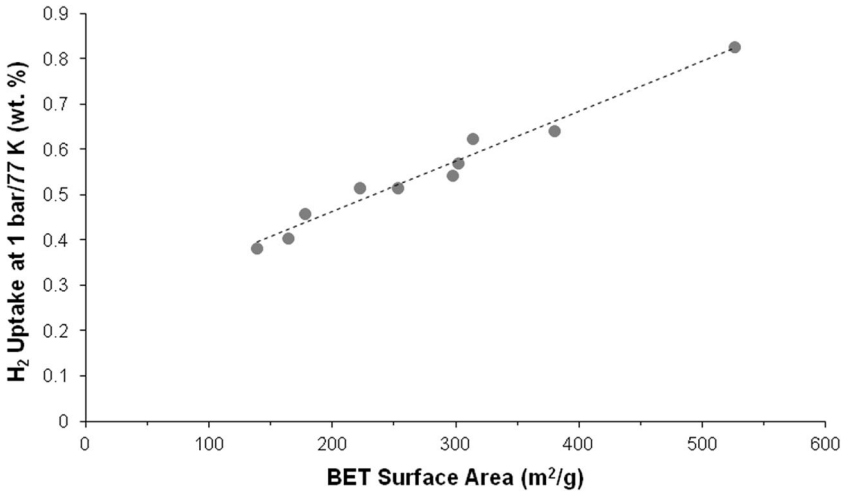

Fig. 7 Plot of the hydrogen uptake at 1 bar/77 K versus the apparent BET surface area of the SNW samples

dramatical change can be understood on the basis of the occurrence of SNW structural changes with DA:MA molar ratio. As previously proved through the comparison of FTIR spectra and elemental analyses values for different SNW samples produced from different DA:MA ratios, the condensation of DA and MA units is completed at DA:MA ratio equal to 1:3 and, below this value, the MA units keep merging into the SNW structure mainly by forming methylene and ether linkages (Scheme 2). Therefore, as the DA:MA ratio decreases from 3:2 to 1:3, more rigid benzene spacer groups (from DA units) are introduced into the network to effectively enhance the porosity and surface area by increasing the network rigidity. When the DA:MA molar ratio decreases to values below 1:3, at which complete condensation of MA and DA units occurs, no further benzene rings are introduced, and MA units are merged into the structure mainly by methylene and ether linkages, leading to a decrease in the surface area of SNW for two reasons. First, methylene and ether linkages are very flexible, thus the network rigidity will decrease. Second, introducing more MA units leads to the presence of more amine-terminated groups, which can easily form hydrogen bonds between the MA-based molecules.

To study the effect of the catalyst amount, many SNW samples were prepared with different DA:Ac molar ratios (Table 2, entries 2 and 6–9). As indicated in Table 2 (and shown in Fig. S2 in Electronic Supplementary Material), the optimum molar MA:Ac ratio was obtained in the range 0.5 to 1. DA:Ac ratios above this range led to a decrease in the surface area, whereas lower ratios were detrimental to surface area in the resulting network.

Generally, the maximum hydrogen uptake at 77 K for different porous materials is correlated with the specific surface area. It has been proved that for all the classes of porous materials, the maximum H_2 uptake is linearly correlated with the apparent BET surface area [8, 56–59]. But in many cases, especially with high BET surface area values (>1,000 m^2/g), this correlation shows a great scatter, and BET surface area is a poor descriptor for H_2 uptake values [13, 60, 61]. In our study, as shown in Fig. 7, we found that a very good linear correlation exists for all data (entries 1–10 of Table 2), suggesting that BET surface area is a good descriptor for the H_2 uptake capacity of these materials.

Finally, the sample SNW-Z (Table 2, entry 10) was prepared according to the procedure described for the SNW synthesis in the experimental part, using now the optimum conditions (DA:MA monomeric molar ratio of 1:3, and DA:Ac molar ratio of 1:1) in order to give the highest surface area of *ca*. 526 m^2/g and hydrogen uptake of 2.57 wt.%, at 77 K and 20 bar.

Conclusions

New SNW porous polymers were prepared, based on Schiff base chemistry, which possess several unique characteristics: a facile one-pot synthesis; cheap and simple monomers and catalyst; high nitrogen content (up to *ca*. 36 wt.%); high thermal stability; and exhibiting gas sorption properties. Several characterization techniques (FTIR spectroscopy, ^{13}C and ^{15}N solid state NMR spectroscopies, and elemental analysis) were used to prove the aminal structure of the synthesized networks with formation of minor methylene and ether linkages.

We have demonstrated that the porosity and hydrogen uptake capacity of these polymers are strongly affected by the monomeric molar ratio and the amount of acidic catalyst used. The newly synthesized polymers exhibit moderate surface areas up to *ca*. 526 m^2/g and moderate hydrogen uptake capacities of 0.82 and 2.57 wt.%, at 77 K, and at 1 and 20 bar, respectively.

The only example known to date of Schiff base networks (SNWs) for H_2 storage applications was reported very recently by Li et al. [39], the corresponding crystalline imine-linked networks showing BET surface areas up to 1,045 m^2/g, and H_2 uptakes of 1.26 wt.% at 77 K, and 1 bar. The H_2 uptake values

obtained by the aminal-linked networks prepared in the present work are very similar to those claimed by Li et al. despite possessing smaller surface areas.

Acknowledgments We thank the Fundação para a Ciência e Tecnologia, Portugal, for financial support (Projects PTDC/EQU-EQU/110313/2009, PEst-OE/QUI/UI0100/2013 and RECI/QEQ-QIN70189/2012) and for a fellowship to C.S.B.G. (SFRH/BPD/64423/2009). We thank the Erasmus Mundus programme (WELCOME) for granting a scholarship to A.G.M. Thanks are also due to Dr. Teresa Nunes for helpful discussions about the solid state NMR measurements.

References

1. Schlapbach L, Züttel A (2001) Nature 414:353–358
2. Yang J, Sudik A, Wolverton C, Siegel DJ (2010) Chem Soc Rev 39: 656–675
3. US Department of Energy, Office of Energy Efficiency and Renewable Energy, and The FreedomCAR and Fuel Partnership, (2009) Targets for Onboard Hydrogen Storage Systems for Light-Duty Vehicles, http://www1.eere.energy.gov/hydrogenandfuelcells/storage/pdfs/targets_onboard_hydro_storage_explanation.pdf
4. US Department of Energy, Stetson N (2013) Hydrogen Storage Program Overview, http://www.hydrogen.energy.gov/pdfs/progress13/iv_0_stetson_2013.pdf
5. Regli L, Zecchina A, Vitillo JG, Cocina D, Spoto G, Lamberti C, Lillerud KP, Olsbye U, Bordiga S (2005) Phys Chem Chem Phys 7: 3197–3203
6. Weitkamp J, Fritz M, Ernst S (1995) Int J Hydrogen Energy 20:967–970
7. Zhao XB, Xiao B, Fletcher AJ, Thomas KM (2005) J Phys Chem B 109:8880–8888
8. Panella B, Hirscher M, Roth S (2005) Carbon 43:2209–2214
9. Meng S, Kaxiras E, Zhang Z (2007) Nano Lett 7:663–667
10. Züttel A, Sudan P, Mauron P, Kiyobayashi T, Emmenegger C, Schlapbach L (2002) Int J Hydrogen Energy 27:203–212
11. Han SS, Furukawa H, Yaghi OM, Goddard WA (2008) J Am Chem Soc 130:11580–11581
12. Germain J, Fréchet JMJ, Svec F (2007) J Mater Chem 17:4989–4997
13. Wood CD, Tan B, Trewin A, Niu H, Bradshaw D, Rosseinsky MJ, Khimyak YZ, Campbell NL, Kirk R, Stöckel E, Cooper AI (2007) Chem Mater 19:2034–2048
14. Wood CD, Tan B, Trewin A, Su F, Rosseinsky MJ, Bradshaw D, Sun Y, Zhou L, Cooper AI (2008) Adv Mater 20:1916–1921
15. Shaffei KA, Atta AM, Gomes CSB, Gomes PT, El-Ghazawy RA, Mahmoud AG (2014) J Polym Res 21:245
16. Belyakova LD, Schevchenko TI, Davankov VA, Tsyurupa MP, Nesmeyanov AN (1986) Adv Colloid Interface Sci 25:249–266
17. Podlesnyuk VV, Hradil J, Králová E (1999) React Funct Polym 42: 181–191
18. McKeown NB, Budd PM (2006) Chem Soc Rev 35:675–683
19. Mackintosh HJ, Budd PM, McKeown NB (2008) J Mater Chem 18: 573–578
20. Schmidt J, Weber J, Epping JD, Antonietti M, Thomas A (2009) Adv Mater 21:702–705
21. Germain J, Fréchet JMJ, Svec F (2009) Small 5:1098–1111
22. El-Kaderi HM, Hunt JR, Mendoza-Cortés JL, Côté AP, Taylor RE, O'Keeffe M, Yaghi OM (2007) Science 316:268–272
23. Campbell NL, Clowes R, Ritchie LK, Cooper AI (2009) Chem Mater 21:204–206
24. McKeown NB, Budd PM (2010) Macromolecules 43:5163–5176
25. Ghanem BS, Msayib KJ, McKeown NB, Harris KDM, Pan Z, Budd PM, Butler A, Selbie J, Book D, Walton A (2007) Chem Commun 67–69
26. Tsyurupa MP, Davankov VA (2006) React Funct Polym 66:768–779
27. Jiang J-X, Su F, Trewin A, Wood CD, Campbell NL, Niu H, Dickinson C, Ganin AY, Rosseinsky MJ, Khimyak YZ, Cooper AI (2007) Angew Chem Int Ed 46:8574–8578
28. Ahn J-H, Jang J-E, Oh C-G, Ihm S-K, Cortez J, Sherrington DC (2006) Macromolecules 39:627–632
29. Hulicova D, Yamashita J, Soneda Y, Hatori H, Kodama M (2005) Chem Mater 17:1241–1247
30. Yang SJ, Cho JH, Oh GH, Nahm KS, Park CR (2009) Carbon 47: 1585–1591
31. Schwab MG, Fassbender B, Spiess HW, Thomas A, Feng X, Müllen K (2009) J Am Chem Soc 131:7216–7217
32. Layer RW (1963) Chem Rev 63:489–510
33. Uribe-Romo FJ, Hunt JR, Furukawa H, Klöck C, O'Keeffe M, Yaghi OM (2009) J Am Chem Soc 131:4570–4571
34. Pandey P, Katsoulidis AP, Eryazici I, Wu Y, Kanatzidis MG, Nguyen ST (2010) Chem Mater 22:4974–4979
35. Ding S-Y, Gao J, Wang Q, Zhang Y, Song W-G, Su C-Y, Wang W (2011) J Am Chem Soc 133:19816–19822
36. Wan S, Gándara F, Asano A, Furukawa H, Saeki A, Dey SK, Liao L, Ambrogio MW, Botros YY, Duan X, Seki S, Stoddart JF, Yaghi OM (2011) Chem Mater 23:4094–4097
37. Uribe-Romo FJ, Doonan CJ, Furukawa H, Oisaki K, Yaghi OM (2011) J Am Chem Soc 133:11478–11481
38. Yang G, Han H, Du C, Luo Z, Wang Y (2010) Polymer 51:6193–6202
39. Li G, Zhang B, Yan J, Wang Z (2014) Chem Commun 50:1897–1899
40. Armarego WLF, Chai CLL (2009) Purification of Laboratory Chemicals. Elsevier Inc, Burlington
41. Marvel CS, Tarköy N (1957) J Am Chem Soc 79:6000–6002
42. Bell RP, Bascombe KN, Coutrey JCM (1956) J Chem Soc 1286–1291
43. Mésangeau C, Yous S, Pérès B, Lesieur D, Besson T (2005) Tetrahedron Lett 46:2465–2468
44. Kailasam K, Jun Y-S, Katekomol P, Epping JD, Hong WH, Thomas A (2010) Chem Mater 22:428–434
45. Coullerez G, Léonard D, Lundmark S, Mathieu HJ (2000) Surf Interface Anal 29:431–443
46. Meier RJ, Tiller A, Vanhommerig SAM (1995) J Phys Chem 99: 5457–5464
47. Larkin P (2011) Infrared and Raman Spectroscopy. Elsevier Inc, Waltham
48. Kaya I, Yildirim M (2009) Synth Met 159:1572–1582
49. Baraka A, Hall PJ, Heslop MJ (2007) React Funct Polym 67:585–600
50. Egger CC, Schädler V, Hirschinger J, Raya J, Bechinger B (2007) Macromol Chem Phys 208:2204–2214
51. Subrayan RP, Jone FN (1996) J Appl Polym Sci 62:1237–1251
52. Hindson JC, Ulgut B, Friend RH, Greenham NC, Norder B, Kotlewski A, Dingemans TJ (2010) J Mater Chem 20:937–944
53. Budd PM, Ghanem BS, Makhseed S, McKeown NB, Msayib KJ, Tattershall CE (2004) Chem Commun 230–231
54. McKeown NB, Gahnem B, Msayib KJ, Budd PM, Tattershall CE, Mahmood K, Tan S, Book D, Langmi HW, Walton A (2006) Angew Chem Int Ed 45:1804–1807
55. Sing KSW, Everett DH, Haul RAW, Moscou L, Pierotti RA, Rouquerol J, Siemieniewska T (1985) Pure Appl Chem 57:603–619
56. Hirscher M, Panella B (2007) Scr Mater 56:809–812
57. Gadiou R, Saadallah S-E, Piquero T, David P, Parmentier J, Vix-Guterl C (2005) Microporous Mesoporous Mater 79:121–128
58. Panella B, Hirscher M, Pütter H, Müller U (2006) Adv Funct Mater 16:520–524
59. Wong-Foy AG, Matzger AJ, Yaghi OM (2006) J Am Chem Soc 128: 3494–3495
60. Thomas KM (2007) Catal Today 120:389–398
61. Nijkamp MG, Raaymakers JEMJ, van Dillen AJ, de Jong KP (2001) Appl Phys A 72:619–623